*energies*

MDPI

*Article*

# Enhancing HVDC Transmission System Reliability Using a Novel Technique for Fault Type Classification and Fault Location Determination

**Walid Mohamed [1,*], Saady Hasan [1], Abdellatif Sayed [1] and Abdelazim Salem [2]**

[1] Electrical Power and Machines Department, Capital University, Cairo 6363040, Egypt
[2] Department of Electrical Engineering, College of Engineering, October 6 University, Giza 3232031, Egypt; abdelazim.salem.eng@o6u.edu.eg
* Correspondence: waledmohamed2112@gmail.com

**Abstract**

Reliable fault detection and accurate fault location are critical challenges in high-voltage direct current (HVDC) transmission systems, particularly under high-resistance fault conditions where conventional protection schemes may exhibit reduced sensitivity. This paper presents a novel protection approach for bipolar HVDC transmission lines based on double-terminal current traveling wave analysis combined with discrete wavelet transform (DWT). The proposed method utilizes current measurements from both the sending and receiving terminals and applies the Daubechies-4 (db4) wavelet to extract high-frequency transient components for fault-type discrimination. Fault location is determined using the arrival times of the first traveling waves at both line terminals. The proposed algorithm is validated using a MATLAB/Simulink model under various fault scenarios, including pole-to-ground and pole-to-pole faults, different fault locations, and high fault resistance values. Simulation results demonstrate that the method accurately identifies fault type and estimates fault location with a maximum error of 0.11%, even for fault resistance up to 100 Ω. Additional analysis confirms robustness under varying operating conditions, transmission line lengths, and noisy measurement signals. Comparative evaluation with recently published methods show that the proposed technique offers improved accuracy, reliability, and suitability for real-time implementation in HVDC protection systems.

**Keywords:** fault detection; fault location; HVDC transmission lines; wavelet transform; voltage source converters

Check for updates

Academic Editor: Constantinos S. Psomopoulos

Received: 24 August 2026
Revised: 6 October 2026
Accepted: 16 October 2026
Published: 9 November 2026

**Copyright:** © 2026 by the authors. Licensee MDPI, Basel, Switzerland. This article is an open access article distributed under the terms and conditions of the Creative Commons Attribution (CC BY) license.

## 1. Introduction

High-voltage direct current (HVDC) transmission systems have become an essential solution for long-distance bulk power transfer, interconnection of asynchronous grids, and integration of renewable energy sources. Compared with HVAC systems, HVDC transmission provides lower losses, improved controllability, and enhanced stability for long-distance applications. However, the protection of HVDC transmission lines remains a significant technical challenge due to the rapid rise in fault current and the absence of natural current zero crossing.

In HVDC systems, fault currents increase rapidly within a very short time, which may cause severe damage to converters, transmission cables, and associated protection equipment. Therefore, fast and reliable fault detection, fault classification, and fault location techniques are essential to ensure system stability and continuity of operation. The challenge

becomes more critical in VSC-HVDC systems because of the high sensitivity of power electronic converters to transient disturbances.

Several methods have been proposed in the literature for HVDC fault protection, including traveling-wave-based methods, wavelet-transform-based approaches, differential protection, and artificial intelligence techniques such as artificial neural networks (ANN), support vector machines (SVM), and k-nearest neighbors (KNN). Traveling-wave methods offer fast response but may require precise synchronization and communication links. Artificial intelligence approaches can achieve high accuracy but generally require extensive training datasets and high computational resources. Wavelet transform has emerged as an effective signal-processing technique due to its capability to capture transient high-frequency components associated with fault events.

Due to the connection between two different grids with different frequencies, it is preferable to connect them through a high-voltage DC transmission line. The sending-end and receiving-end DC voltages are obtained using voltage source converters (VSC) with high-voltage direct current; these voltage sources are obtained by converting high-voltage alternating current (HVAC) to HVDC by using fully controllable power electronic converters to enable changing the value of the voltage at both ends of this line, then controlling the direction of power flow from one end that has the larger voltage to the other end. There are some issues that have an impact on this operation that must be included for the HVDC transmission system, such as the increased demand of one grid connected at the first end of this HV line from the other grid connected to the second end, frequent power outages, power quality issues, and which lead many utility customers to look for alternative energy sources.

It is necessary to protect transmission lines with great precision, as direct current transmission lines are widely used in connecting electrical networks of different frequencies, and with the great progress in modern technologies for detecting network faults, it is necessary to immediately disconnect the fault. It has been shown that when a fault occurs in DC circuits, the fault current in the damaged cable increases linearly [1], while in the healthy cable, it increases cubically within a few seconds. Based on this, a method was proposed to detect the fault by the average value of the current. This method focuses on the region of increased high frequencies in the network. But it is applied to a fault detection algorithm for a multi-terminal line-commutated converter with infinite synchronous generators, called an interconnected grid system. The HVDC Interconnected Grid is dependent on obtaining the second derivative of the faulty DC current of any pole, which shows the acceleration of the DC current [2]. New techniques based on ANN for fault detection are reviewed for high-voltage direct current HVDC transmission lines; three stages of neural networks are used: first, a neural network that receives samples of direct current, the second neural network receives frequencies, and the third network uses current values and changes them over time [3–5]. The first network is used to determine whether there is a fault or not by taking current samples and comparing the network output with the current values in the normal state. If a fault is proven, the fault current values are sent to the second neural network to determine the type of fault. After determining the type, the values are sent again to the last network to determine the location of the fault and completely isolate the location of the fault. This method is considered accurate, but it is relatively complex and requires extensive training cycles to be built. It uses a wavelet transform to describe a Comparative Analysis of fault detection using standard deviation [6]. This method uses the advanced technique of wavelet multiresolution analysis. In the case of faults, this method helps in analyzing the waveforms resulting from the fault to determine the different frequencies that occur as a result of this fault; by applying standard deviation to the mother wavelet, this technique shows that Db4 is the accurate mother wavelet to estimate the fault. In Ref. [7], a method for restricting and controlling fault current using a variable resistive bridge controller was proposed, along with an algorithm based on a fuzzy logic

controller; this method introduces dynamic resistance into the circuit when a fault occurs. This helps to limit the fault current and reduce its effects, improving system reliability. The innovation is improved by activating the fault-current control using the HCLID device, which injects an opposing DC through a charged capacitor. A variable resistance is used to resist the fault current, while a switch is used to disconnect the fault current at a given time [8]. This method is based on superconducting residual current limiters (SFCLs) to protect HVDC systems. This method offers fast current limiting and is called a hybrid fault current limiter and interrupting device (HCLID). This device is a solid-state commutation circuit that is used to inject counter current from a stand-by recharged capacitor and core reactor as a limiting device and fast contact; all these components are connected in parallel. A Hilbert transform is a transformation of waves from one waveform to another waveform associated with the same new original waveform, allowing information from the waveform to be transmitted without being affected by any noise. The Hilbert transform was used to detect faults and distinguish between internal and external faults in high-voltage direct current [9]. The technique is applied to voltage and current to calculate the reactive power. The value of the specified instantaneous reactive power is determined by multiplying the current and voltage; then by integrating the reactive power, the reactive energy is produced. By calculating the reactive energy on the rectifier side and the inverter side, the fault can be identified, and its type can be determined. The stationary wave transform is also a wave analysis technique because it is distinguished from the Hilbert transform by its ability to remove noise and analyze waves at different frequencies. It was suggested that the stationary wave transform be used as an additional protection instead of relying only on the traditional method of protection [10]. First, using the current signal removes the noise in the signal and uses a correlation indicator. Between the currents of the rectifier and the inverter, if the correlation signal is positive, it means a pole-to-pole fault, and if it is negative, it is a positive or negative pole fault. The method of transforming waves using the fast Fourier transform differs from the Hilbert transform and the stationary wavelet transform in that it transforms the wave from the time domain to the frequency domain, which means breaking the wave into a group of waves. This method becomes useful in the case of a wave with different frequencies or frequent changes. In [11–13], it was suggested to use the Fourier transform, specifically the use of Radix-2 DIT, due to its effectiveness and speed in processing data. When an electrical fault occurs, a high frequency appears, which differs from the frequency of the wave in the normal case. By converting the wave to the frequency domain, the fault can be detected. New methods have been developed to detect faults that no longer require wave analysis before detecting the fault or waiting for a short time to determine whether the permanent or transient fault, but it requires pre-training to collect data. Machine learning using data is one of the methods that have been proposed to identify the fault without the need to analyze the waves [14–16]. It deals directly with the original wave. A method has been proposed to detect faults using SVM and KNN for self-learning using the voltage wave. When a fault occurs, a set of values from the voltage wave is collected. Using the KNN algorithm compares the current values with values collected during training from the voltage wave to determine the type of fault by comparing the values to each other to determine the fault after knowing the extent of the proximity between the new values and the collected values. As for the SVM, it separates the collected values by drawing a separate drawing for each set of values and determining the type of fault for it. When reading new values, it studies where these values are in the drawing to detect the fault. A method was proposed to detect faults using a voltage-controlled oscillator with a smooth reactor by observing changes in voltage. When a fault occurs, the voltage value on the smooth reactor is monitored and sent to the voltage-controlled oscillator [17]. When the voltage value exceeds a specified value, a signal is sent to the circuit breaker to disconnect the fault. This presents a study and analysis of VSC-HVDC in a pole-to-pole fault. Another

one of the most important types of machine learning is support vector machines (SVM), which is a technique that also requires prior training to collect data [18–20]. The applied technology depends on voltage data collected during training, and the method continuously monitors changes in the voltage to measure the extent to which the values belong to the values that were collected [21]. This method depends on collecting the voltage or current data from one side, whether the rectifier or the inverter, so there is no need for communication between the two sides. Traveling waves are electrical waves that travel through wires or transmission towers because of a change in current or voltage due to a specific fault. These waves travel from the fault point to all parts of the system in the form of shock waves. A technique was proposed to use traveling waves to detect faults. When a fault occurs, shock waves are generated when the current and voltage values reach a local station [22]. The change in transient energy is observed. When they exceed a specified value, this indicates the presence of a fault. The affected pole is identified by deriving the current for each pole. Many protection methods have failed to distinguish between fault currents and transient currents [23–26]. Transient waves have also been used to distinguish between fault currents and transient currents by using the speed of wave transmission and waiting for a time to determine whether the fault current is temporary or permanent. The fault current shows a large time difference between the two currents in the poles with a difference in polarity, while the transient current does not cause a large change or a change in polarity. A new method was developed to detect faults using Levenberg–Marquardt deep learning [27]. The voltage is monitored until a drop occurs because of a fault. This value is compared with other values that were taken, and the neural network makes the decision whether to disconnect if the fault is permanent. Mathematical methods are one of the most important methods for detecting faults. Differential current protection was used. This method depends on finding the difference between the two currents in the rectifier and inverter directions. However, this method is ineffective in the event of faults with high resistance [28].

Although wavelet transform has been widely used in HVDC protection studies, most existing methods focus either on fault detection only or require complex communication and signal processing schemes. The novelty of this work lies in integrating discrete wavelet transform with double-terminal current traveling wave analysis to simultaneously perform fault type classification and accurate fault location using a simple and computationally efficient algorithm. Unlike machine-learning-based approaches, the proposed method does not require prior training data and maintains high accuracy even under high-resistance faults.

The present study focuses on DC faults in bipolar HVDC transmission lines, specifically pole-to-ground and pole-to-pole faults. LLL (three-phase line-to-line) and LLLG (three-phase line-to-line-to-ground) faults are AC faults that occur on the AC side of the converter transformers, not on the DC transmission line itself. Since the proposed protection scheme is designed specifically for the DC transmission line, AC-side faults are handled by conventional AC protection devices (e.g., distance relays, differential protection) located on the AC side.

*The Main Contributions of the Proposed Technique*

The proposed technique is applied as a new criterion for the evaluation of the protection system that must verify selectiveness, responsiveness, and reliability. In addition, the applied algorithm uses transient characteristics for distance protection based on wavelet transform ́which uses the two current signals of the positive and negative poles of the HVDC transmission line to find the detailed coefficients of these currents. The technique is used to identify the type of fault and determine the location of the fault; the main contributions of the proposed technique are summarized as follows:

(a) The presented technique applies wavelet transform (WT) to current signals to obtain the detailed coefficients in both faulty and normal conditions.

(b) It is tested on Matlab/Simulink model for a bipolar HVDC transmission line.
(c) The fault type discrimination and fault location are determined with effectively accurate obtained results.
(d) The location of the fault is successfully estimated by the proposed scheme, even if the fault has higher resistance.
(e) The proposed method is evaluated using a bipolar VSC-HVDC simulation model with the specified operating voltage and 75 km transmission-cable length. Its applicability to other voltage levels, line lengths, and transmission configurations requires further investigation.
(f) A Simulink model is introduced to demonstrate the proficiency of the presented method.

Unlike conventional wavelet-based protection methods that mainly focus on fault detection only, the proposed method integrates both discrete wavelet transformation and double-terminal traveling wave analysis to simultaneously determine fault type and fault location in bipolar HVDC transmission lines. The proposed approach uses both positive and negative pole current signals at sending and receiving terminals, which improves selectivity and sensitivity under high-resistance fault conditions. In addition, the presented algorithm achieves accurate fault location without requiring complex training datasets or computationally intensive optimization techniques, making it suitable for practical real-time implementation.

## 2. Research Methodology

The HVDC transmission line is a DC link between two electrical power systems, where they operate at a voltage of 230 kV and a rated apparent power of 200 MVA, but their operating frequencies are 50 Hz and 60 Hz, respectively. The HVDC link has a rated power and voltage of 200 MVA and ± 100 kV. To evaluate the performance of the proposed method, a comprehensive simulation model was developed in MATLAB/Simulink utilizing the Simscape Power Systems library. The components, including [the two power systems, transformers, rectifier, inverter and HVDC transmission lines], were modeled to reflect realistic grid conditions. The DC line power flow is from the first power system, which contains a rectifier, to the second power system, which contains an inverter; this DC link is a cable of 75 km and includes two smoothing reactors of 8 m H. Two converters located at the two ends of the line are equipped with IGBT-based three-level NPC technology and apply the concept of PWM that produces a carrier waveform that has a frequency equal to 27 times the fundamental frequency.

Each power system is connected to the DC link through a step-down star-earthed delta transformer AC filter, a reactor on the AC side, and DC sides composed of DC filters and capacitors. The model uses VSC control, as illustrated in Figure 1, which provides the configuration of each power system source. To regulate the converter's real and reactive power outputs, by setting converter reactors and leakage reactance of transformer to 0.15 pu to adjust the VSC output voltage in both phase and magnitude at the Point of Common Coupling.

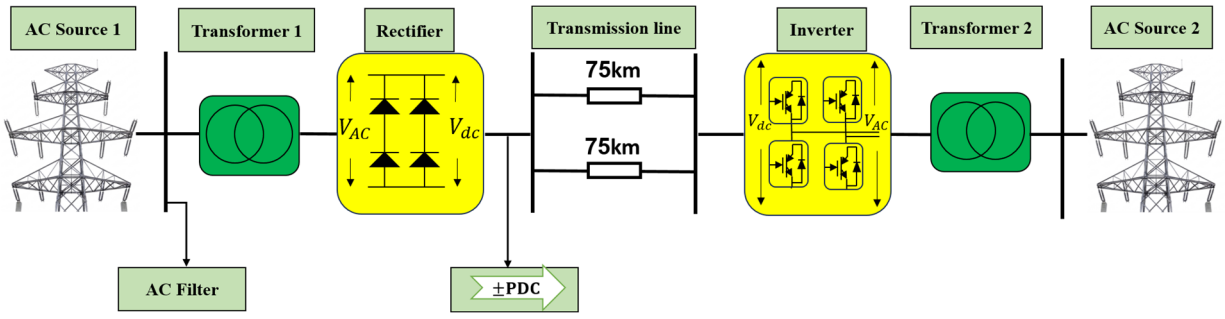


**Figure 1.** Block diagram of a VSC-HVDC link.

## 3. Fault Classification Algorithm

HVDC transmission lines are widely used for interconnecting asynchronous power systems, integrating renewable energy sources, and enabling long-distance bulk power transfer. However, these systems are highly vulnerable to DC faults because of the rapid increase in fault current and the absence of natural current zero crossing. Therefore, a fast and reliable protection scheme is essential to detect the fault, classify its type, and accurately determine its location.

The proposed protection algorithm is based on the analysis of transient current signals measured at both terminals of the bipolar HVDC transmission line. When a fault occurs, a sudden change in current generates high-frequency traveling waves that propagate along the transmission line toward both terminals. These transient components contain significant information about fault occurrence and can be effectively extracted using the discrete wavelet transform (DWT).

In this study, the measured positive pole current, negative pole current, and ground current are processed using the Daubechies-4 (db4) wavelet. The DWT decomposes each signal into approximation and detail coefficients. The detail coefficients at the first decomposition level are used because they capture the initial high-frequency transients generated immediately after fault inception.

The first-level decomposition was selected after comparative investigation because it provides the highest sensitivity to abrupt changes in current while minimizing computational burden. Higher decomposition levels contain lower-frequency components and were found less effective for immediate fault detection.

The maximum absolute value of the detail coefficients is calculated for each pole current. Under normal operating conditions, these coefficients remain very small due to the absence of sudden transients. When a fault occurs, the corresponding faulted pole exhibits a significant increase in the detail coefficient magnitude. Therefore, by comparing the maximum coefficient values with a predefined threshold, the fault type can be identified.

The threshold value was set to 500 after extensive simulation under normal and fault conditions. During healthy operation, all detailed coefficients remained below this value, whereas all fault cases produced values significantly greater than the threshold. This ensures reliable discrimination between normal and faulty states without false tripping.

The classification criteria are summarized as follows:

If the positive pole coefficient exceeds the threshold while the negative pole remains below it, the fault is classified as a positive pole-to-ground fault.

If the negative pole coefficient exceeds the threshold while the positive pole remains below it, the fault is classified as a negative pole-to-ground fault.

If both positive and negative pole coefficients exceed the threshold simultaneously, the fault is classified as a pole-to-pole fault.

To improve feature extraction and decouple the coupled pole currents, Clarke transformation is applied to convert the original pole currents into modal components. The modal components allow better identification of traveling wave signatures for different fault conditions and improve the accuracy of fault location estimation.

The transformed modal currents are subsequently analyzed using the db4 wavelet to determine the arrival times of the first traveling waves at both line terminals. These arrival times are then used in the fault location algorithm described in the following section.

HVDC transmission line is essential for connecting two power system grids that operate with different frequencies, and it is also used for smart grids and renewable energy applications on a large scale. Nevertheless, DC transmission systems are more susceptible to faults than AC transmission systems, as in Refs. [29–32] that occur due to the detrimental effects of DC resistances and the sensitivity of power electronics modules used for converting from AC to DC power systems. The large magnitude and sudden increase in fault

current make fault detection, isolation, and ensuring reliable operation in high-voltage DC transmission lines highly challenging. Selection of a suitable protection system must ensure the system's continuity of operation and mitigate and reduce damage resulting from the fault that occurred. One of the most modern advanced techniques used for signal analysis is called multi-resolution analysis (MRA), which is applied to analyze the transient signals of fault current, particularly at different frequencies that may occur with these transient signals. This technique allows for the dismantling of a signal into multiple frequency bands; the application of this technique is a highly effective tool for identifying electrical faults in HVDC systems. However, this method is sensitive to high-frequency noise, which may be stacked on the signal. Better analysis of the MRA method requires information on decomposition levels and efficiently assesses signal quality. In the proposed method, for any signal x(t), it can be decomposed into approximation and detail coefficients, estimated and specific coefficients depicted by the scaling $G_{m,n}(t)$ and the wavelet function $\mathrm{H}_{m,n}(t)$, respectively.

$$G_{m,n}(t) = 2^{-(\frac{m}{2})}\, \emptyset(\, 2^{-m}(t - n\,)) \tag{1}$$

$$\mathrm{H}_{m,n}(t) = 2^{-(\frac{m}{2})}\, \emptyset(\, 2^{-m}\,(t - n)) \tag{2}$$

Scaling function $G_{m,n}(t)$: Used to illustrate components of low frequency of the signal.

Wavelet function $\mathrm{H}_{m,n}(t)$: Used to illustrate the components of high frequency or details of the signal.

The wavelet transform is linked to the high-pass filter, and the scaling function is linked to the low-pass filter H(n) due to G(n) obtained from the following Equations (3) and (4), respectively.

$$M(t) = \sqrt{2}\sum_{n} \mathrm{H}(n)\; G(2t - n) \tag{3}$$

$$\mathrm{N}(t) = \sqrt{2}\sum_{n} \mathrm{G}(n)\; \mathrm{H}(2t - n) \tag{4}$$

As shown in the following Figure 2, the high-pass filter generates the coefficients $D_i$ which illustrate the high-frequency component and its details, whereas the low-pass filter generates the coefficients $A_i$ which illustrate the low-frequency component and its details.

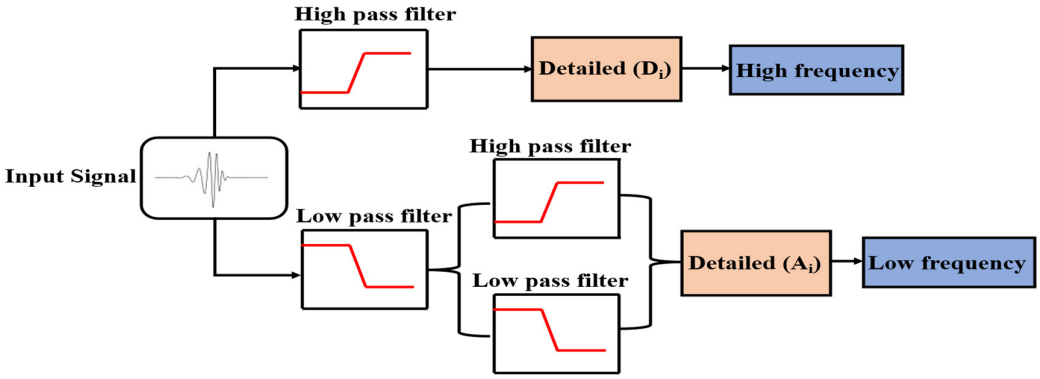


**Figure 2.** Signal WT decomposition.

The initial step involves passing the original signal through both filters to obtain the detail coefficients $D1$ and the approximation coefficients $A1$ for l equal 1 (with scale a equal $2^1$). Following the removal of a factor of 2, coefficients $A1$ are filtered again to produce.

This process is repeated with the reduced approximation coefficients $A2$ to obtain subsequent levels of coefficients, as depicted in Figure 2.

In this study, the first decomposition level (D1) of the discrete wavelet transform is utilized because it captures the initial high-frequency transient components generated immediately after fault occurrence. These components contain the most significant information

for fault detection and classification. Higher decomposition levels were examined; however, they showed reduced sensitivity to the fast transients associated with HVDC line faults.

The Daubechies-4 (db4) mother wavelet was selected after comparative testing with db2, db6, and Symlet families. The db4 wavelet provided the best compromise between time localization and frequency resolution, enabling clearer detection of traveling wave transients while maintaining computational simplicity.

The VSC employs PWM switching at 27 times the fundamental frequency (i.e., 1350 Hz for a 50 Hz system and 1620 Hz for a 60 Hz system). These switching operations introduce high-frequency ripples into DC current. However, the proposed method is robust to this effect because:

1. The switching ripple is periodic and steady state, whereas fault transients are impulsive and broadband.
2. The db4 wavelet's first-level detail coefficients capture the abrupt, non-periodic transient associated with fault inception, while the periodic switching ripple produces relatively small and consistent detail coefficients that remain below the threshold.
3. The results were verified through simulation, showing that the maximum detail coefficients during normal converter switching operation remain below 250, well below the threshold of 500.

*Fault Location Algorithm*

HVDC transmission systems are used as a preferable solution for long–distance transmission, and the power systems operate with high ratings. So, these systems are important to protect effectively. The proposed technique depends on the analysis of traveling waves that appear at both ends of the line after the occurrence of a fault; this principle of traveling waves that go online from the position of the fault to the line ends plays a crucial role in determination of the fault location.

By using the arrival times of the first reflected waves at both ends, the position of the fault is determined. This technique is applied to the presented model for determination of fault location, which verifies accurate results as illustrated in the following sections.

Figure 3 shows a schematic diagram of an HVDC line with a positive-to-negative pole fault scenario. The proposed technique is illustrated for this case and other types of faults for recognizing and locating the faults.

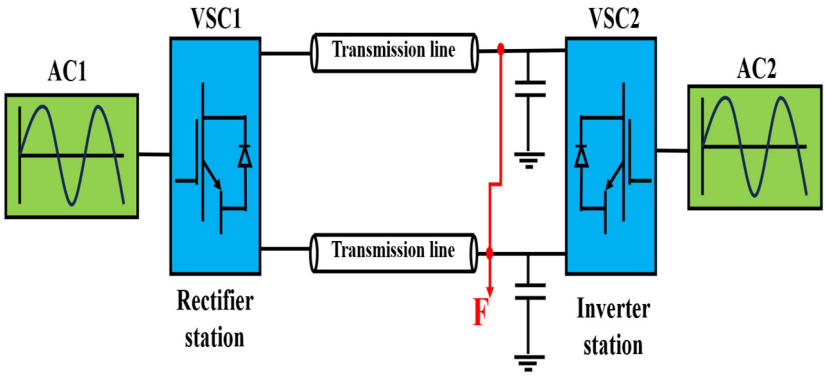


**Figure 3.** Positive-to-negative pole fault in HVDC line section.

After the fault occurs, many sudden changes happen as a fault occurs in the system, which produces traveling waves of current and voltage that propagate in the two directions along the transmission line from the faulted point as shown in Figure 4. These waves travel until they reach a point that has a different characteristic impedance from that of the faulted line; this will happen at line end terminals and intersections. The traveling waves online

have forward and backward waves; the forward-traveling waves of voltage and current can be expressed as:

$$V_f(x,t) = V_0\, e^{j(wt-\beta x)} \tag{5}$$

$$I_f(x,t) = \frac{V_0}{Z_0}\, e^{j(wt-\beta x)} \tag{6}$$

where $V_0$ is the value of the voltage before the fault at the faulted point, $w$ is the angular frequency, β is propagation constant, and $Z_0$ is the characteristic impedance of the line.

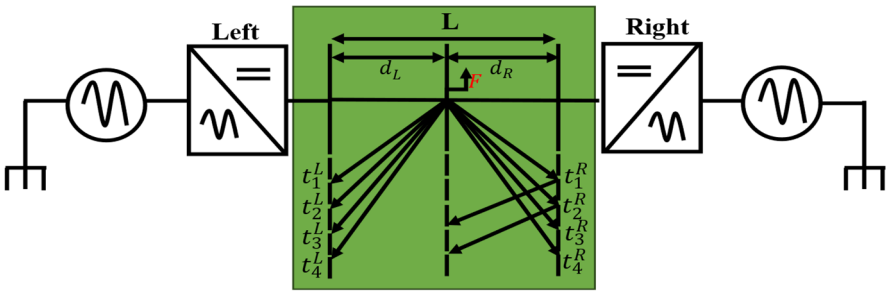


**Figure 4.** Lattice illustration of a fault in a transmission line.

While the backward-traveling waves for voltage and current can be written as:

$$V_b(x,t) = V_1 e^{j(wt\,+\,\beta x)} \tag{7}$$

$$I_b(x,t) = \frac{V_1}{Z_0} e^{j(wt+\beta x)} \tag{8}$$

where $V_1$ is the value of voltage at the reflected position; then the total voltage and current on the line after the first reflection can be obtained as the summation of forward and backward waves from the following equations.

$$\mathrm{V(x,t)} = V_f(\mathrm{x,t}) + V_b(\mathrm{x,t}) = V_0\, e^{j(wt-\beta x)} + V_1 e^{j(wt+\beta x)} \tag{9}$$

$$\mathrm{I(x,t)} = \frac{V_0}{Z_0} e^{j(wt-\beta x)} - \frac{V_1}{Z_0}\, e^{j(wt+\beta x)} \tag{10}$$

For positive pole, negative pole and ground forward-traveling wave currents are expressed as:

$$I_P(x,t) = \; e^{j(wt-\beta x)} \mathrm{X} I_{P0} \tag{11}$$

$$I_N(x,t) = e^{j(wt-\beta x)} \mathrm{X} I_{N0} \tag{12}$$

$$I_G(x,t) = e^{j(wt-\beta x)} \mathrm{X} I_{G0} \tag{13}$$

where $I_{P0}$, $I_{N0}$ and $I_{G0}$ are currents before the fault.

The backward-traveling wave currents after the fault can be articulated as:

$$I_P(x,t) = \; e^{j(wt\,+\,\beta x)} \mathrm{X} I_{P1} \tag{14}$$

$$I_N(x,t) = e^{j(wt+\beta x)} \mathrm{X} I_{N1} \tag{15}$$

$$I_G(x,t) = e^{j(wt+\beta x)}\; \mathrm{X} I_{G1} \tag{16}$$

where $I_{P1}$, $I_{N1}$ and $I_{G1}$ are currents after the fault.

When positive pole-to-negative pole fault occurs on HVDC line, that represent is a symmetrical fault. Applying Clarke's transformation to obtain the following components of currents $I_\alpha$, $I_\beta$, and $I_0$ from the positive, negative, and ground currents as illustrated by Equation (17).

$$\begin{bmatrix} I_\alpha \\ I_\beta \\ I_0 \end{bmatrix} = \frac{1}{3} \begin{bmatrix} 2 & -1 & -1 \\ 0 & \sqrt{3} & -\sqrt{3} \\ 1 & 1 & 1 \end{bmatrix} \begin{bmatrix} I_P \\ I_N \\ I_G \end{bmatrix} \quad (17)$$

where $I_\alpha$, $I_\beta$ and, $I_0$ are the modal current components, and applying wavelet transform the inception and arrival times of the current traveling waves at the fault location framework can be determined. This paper employs the db4 wavelet for this objective.

Where $I_P$, $I_N$, and $I_G$ represent the positive pole, negative pole, and ground currents, respectively. The modal transformation decouples the coupled pole currents into independent components, which improves fault feature extraction for different fault types.

Wavelet decomposition includes breaking down the original signal into estimated and detail components, each of which can be further decomposed for improved resolution. For this study, the details from the first-level detail coefficients are employed. Consequently, using the Daubechies-4 wavelet (db4), the alpha modal component of the current signal is changed, and the initiation of traveling waves at the fault locator is recognized through the details of the decomposition.

As shown in Figure 5, the method reads the current values ($I_P$, $I_N$, and $I_G$) for the positive, negative, and ground poles, respectively, then calculates the maximum coefficient value for each pole (P, N, and G) and compares it with the base current value, which is set at 500. If the maximum coefficient value for the positive pole exceeds 500, the fault is a positive-ground fault, and likewise for the negative pole and ground. The fault location is determined using the measured current values and using the Clark transform and wavelet transform the fault location is determined accurately.

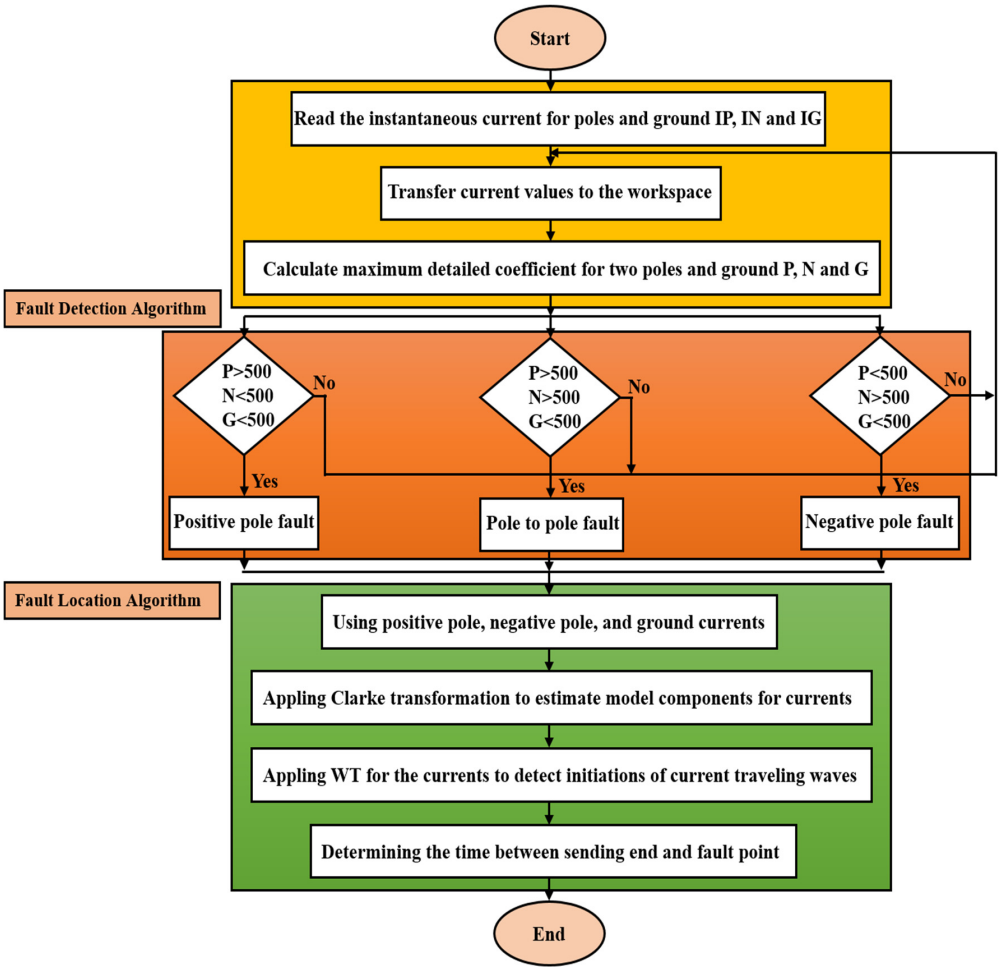


**Figure 5.** The flowchart of the proposed methodology.

The DWT decomposition is implemented using complementary low-pass and high-pass analysis filters. The low-pass filter retains the lower-frequency components of the current signal, whereas the high-pass filter extracts the high-frequency transient components associated with fault disturbances. The cutoff frequencies and corresponding frequency bands are determined according to the selected sampling frequency and decomposition level. The detailed coefficients containing the most significant fault-related transient information are subsequently used for fault identification.

The threshold value used for fault discrimination was selected based on repeated simulation under normal and fault conditions. During normal operation, the maximum detailed coefficients of the analyzed pole currents remained below 250 for all tested cases. Under fault conditions, the minimum observed detailed coefficient exceeded 480. Therefore, a threshold of 500 was selected as a secure discrimination criterion to avoid false operation while ensuring reliable fault detection.

This threshold can be adapted for other system ratings by normalizing the current signals measured to the base current of the HVDC system studied.

## 4. Simulation Results and Discussion

The model is tested on MATLAB/Simulink 2018b that is shown in Figure 1, under many case studies. Assume the direction of current is from the power system that operates as a rectifier converter, and then the power flow is assumed positive when entering the converter. The test cases are shown as follows. All the test cases are charted for time from t = 0 s to t = 5 s.

Figure 6 shows the current of the positive and negative poles when the simulation system is operated under normal operation without fault.

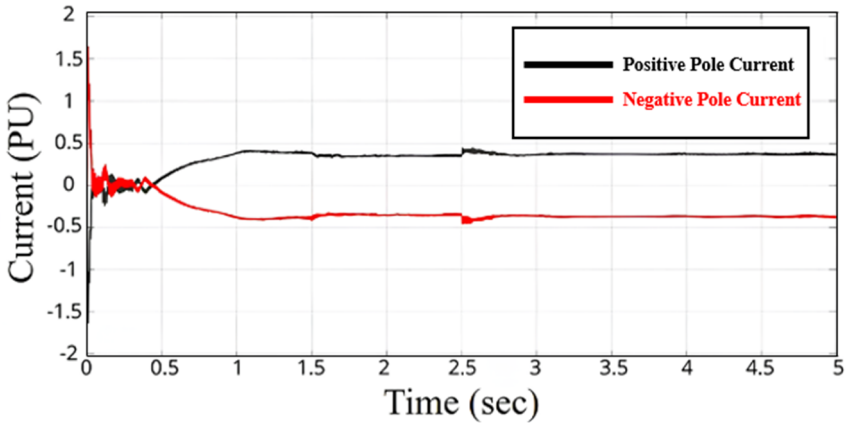


**Figure 6.** Positive and negative per-unit pole currents.

The system may be subject to three types of faults that may occur, which are positive pole to ground, negative pole to ground or pole-to-pole faults.

The instantaneous values of the positive and negative pole currents are shown in Figure 7a–c during different types of faults: negative pole to ground, positive pole to ground and pole-to-pole fault, respectively. The value of the fault pole current increased.

The proposed technique responses are shown in Table 1. As explained before, the maximum coefficient values of positive pole (m), negative pole (n) and ground ($p$) will be changed from the normal values, according to the type of fault, while the value of the maximum coefficient value of positive pole (m) will be increased during positive pole to ground fault, as same as during negative pole to ground fault the maximum coefficient value of negative pole (n) will be increased, and the two values will be increased during

pole to pole fault. The results obtained for maximum coefficient value for the different operating and fault conditions are illustrated in Table 1.

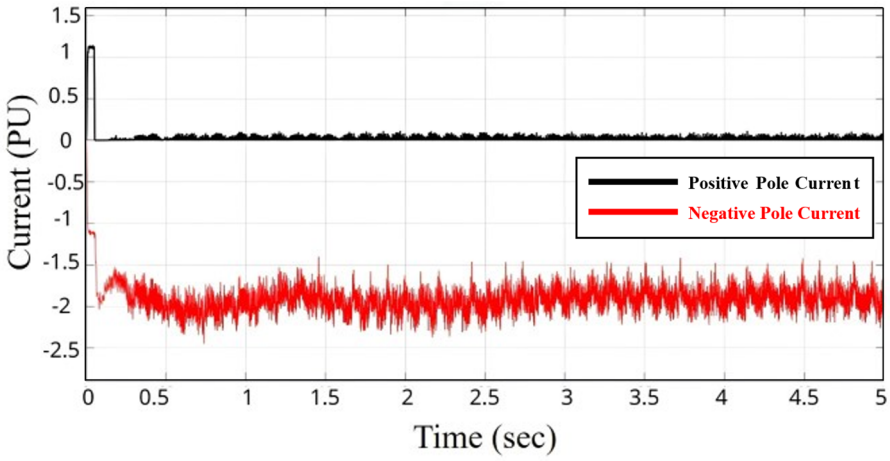


(**a**) The instantaneous values of positive and negative pole per unit currents during negative pole fault

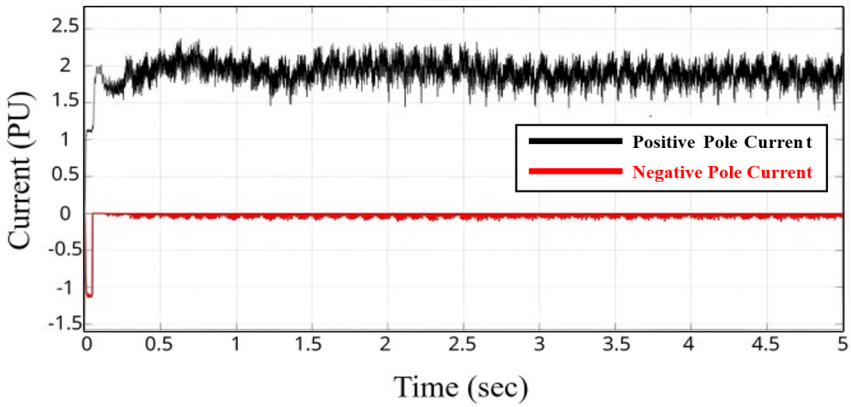


(**b**) The instantaneous values of positive and negative pole per unit currents during Positive pole fault

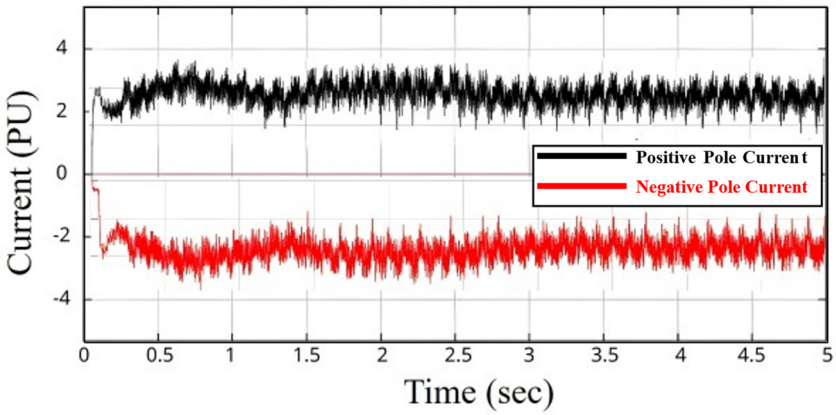


(**c**) The instantaneous values of positive and negative pole per unit currents during pole-to-pole fault

**Figure 7.** The instantaneous values of Positive and negative per-unit pole currents for different types of faults.

In practical HVDC systems, DC current measurements are subject to harmonics, ripple, sensor error, and noise. To evaluate the robustness of the proposed DWT-based fault classification under measurement errors and noise, this methodology is characterized by applying the db4 wavelet, which acts as a band-pass filter that effectively isolates the high-frequency transient components associated with fault inception while attenuating low-frequency ripple and steady-state harmonics. It is also clarified that the threshold of

500 provides a wide margin because of the results in normal operation coefficients $< 250$; while in case of fault, the coefficients $> 480$, which ensures reliable discrimination even under realistic measurement errors.

**Table 1.** Maximum coefficient value for the different operating and fault conditions.

| Type of Fault | Max. Coefficient of Positive Pole (m) | Max. Coefficient of Negative Pole (n) | Max. Coefficient of Ground ($p$) |
|---|---|---|---|
| Normal operation | 0.2328 | 0.2328 | $9.0650 \times 10^{-14}$ |
| Positive pole to ground fault | $4.8322 \times 10^{3}$ | 233.3555 | $1.6234 \times 10^{-12}$ |
| Negative pole to ground fault | 27.8076 | $1.3395 \times 10^{4}$ | $2.0831 \times 10^{-12}$ |
| Pole to pole fault | $4.8166 \times 10^{3}$ | $1.5379 \times 10^{4}$ | $2.8154 \times 10^{-13}$ |

From the presented results, when a fault occurs in any pole, its maximum coefficient value increases, so the type of fault is determined.

Table 2 illustrates the effect of changing the fault resistance value on the proposed technique response. The presented results demonstrate that the technique successfully identified the fault type despite changes in the fault resistance value.

**Table 2.** Effect of fault resistance changing on the maximum wavelet coefficient values during a positive pole-to-ground fault.

| Fault Resistance | Max. Coefficient of Positive Pole (m) | Max. Coefficient of Negative Pole (n) | Max. Coefficient of Ground ($p$) |
|---|---|---|---|
| 0 | $4.8322 \times 10^{3}$ | 233.3555 | $1.6234 \times 10^{-12}$ |
| 10 | $3.5697 \times 10^{3}$ | 189.021 | $1.01 \times 10^{-12}$ |
| 50 | $2.1125 \times 10^{3}$ | 99.580 | $0.999 \times 10^{-12}$ |
| 100 | $1.2140 \times 10^{3}$ | 50.235 | $0.87 \times 10^{-12}$ |
| 500 | 330.21 | 10.998 | $0.465 \times 10^{-12}$ |
| 1000 | 100.505 | 4.2350 | $0.1118 \times 10^{-12}$ |

Table 3 illustrates the effect of changing the fault location on the proposed technique's response. The presented results demonstrate that the technique successfully identified the fault type despite changes in fault location.

**Table 3.** Effect of fault location on the maximum wavelet coefficient values during a positive pole-to-ground fault.

| Fault Location (km) | Max. Coefficient of Positive Pole (m) | Max. Coefficient of Negative Pole (n) | Max. Coefficient of Ground ($p$) |
|---|---|---|---|
| 5 | $9.8975 \times 10^{3}$ | 652.35 | $2.2321 \times 10^{-12}$ |
| 10 | $7.0122 \times 10^{3}$ | 456.50 | $1.9875 \times 10^{-12}$ |
| 20 | $6.0059 \times 10^{3}$ | 356.88 | $1.8725 \times 10^{-12}$ |
| 40 | $5.0971 \times 10^{3}$ | 299.74 | $1.7959 \times 10^{-12}$ |
| 60 | $4.9911 \times 10^{3}$ | 256.21 | $1.6989 \times 10^{-12}$ |
| 75 | $4.8322 \times 10^{3}$ | 233.3555 | $1.6234 \times 10^{-12}$ |

The results in Table 3 show that the maximum wavelet coefficient of the positive pole decreases as the fault location moves farther from the measuring terminal. This behavior indicates that the sensitivity of the wavelet-coefficient-based fault criterion is dependent on the fault distance. In particular, the coefficient obtained at 500 km is lower than that obtained for the shorter distances considered. Therefore, the results at extended distances should be regarded as a sensitivity study rather than evidence that the proposed criterion maintains the same detection margin for transmission lines of arbitrary length. The complete fault classification and fault-location validation presented in this study are based on the 75 km HVDC system model.

## 5. Proposed Mechanism for Fault Location

According to the principle of traveling waves, due to the occurrence of a fault on the HVDC transmission line, there are two traveling waves that go to both ends of this line from the position of the fault, as illustrated in Figure 8. By determining the consumed time taken for the first incident traveling waves at both ends, the location of the fault from the sending end of the line can be determined according to the following Equations (18)–(21). The location of the fault depends on the interval between the timing of the first incident waves at the sending end and the receiving end, as explained below:

- The fault is located at a distance less than half the line length if this interval is positive.
- The fault at distance is greater than the middle of line length if this interval is negative.
- But the fault at the middle of line length, if the two times at sending and receiving end equally.

$$\begin{cases} T_1 = \frac{X}{V} \\ T_2 = \frac{L-X}{V} = T - T_1 \\ T = \frac{L}{V} \end{cases} \quad (18)$$

$$T_2 - T_1 = T - 2T_1 = T - 2X\frac{X}{v} = T - (T_2 - T_1) \quad (19)$$

$$X = \frac{V\,XT}{2} - \frac{V}{2}X(T_2 - T_1) \quad (20)$$

$$X = \frac{L}{2} - \frac{1}{2}XVX(T_2 - T_1) \quad (21)$$

where

X: Fault location from sending end
L: Total length of line
V: Propagation waves velocity
$T_1$ & $T_2$: the arrival times of the first incident traveling waves after fault occurrence, measured at the sending and receiving ends, respectively.

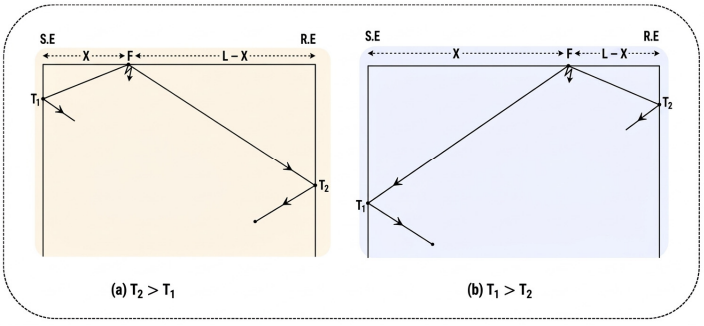


**Figure 8.** Working principle for determination of fault location.

The calculated error associated with the estimated fault location distance can be found using the following equation:

$$\text{Error} = \frac{|\text{obtained fault location} - \text{actual fault location}|}{\text{actual fault location}} \times 100 \quad (22)$$

## 6. Fault Location Algorithm Results

When a fault has occurred in HVDC transmission lines, the amplitude of the current increases rapidly and the determination of fault location is determined by the proposed technique with high accuracy when applying many case studies for the three types of faults, positive pole-to-ground, negative pole-to-ground and pole-to-pole faults, with different values of fault resistances.

In this section, the accuracy of the proposed algorithm for determination of fault location, and the effect of large fault resistance on the errors of the proposed technique relative to previous research will be presented.

Table 4 presents the accuracy of the proposed algorithm for determination of fault location.

**Table 4.** Accuracy of the proposed algorithm for determination of fault location.

| Fault Type | Actual Distance (km) | Estimated Distance (km) | The Absolute Error (km) | The Error % |
|---|---|---|---|---|
| Pole-to-pole | 75 | 75 | 0.004 | 0.0055 |
| | 50 | 49.98 | 0.016 | 0.0319 |
| | 25 | 24.97 | 0.026 | 0.1059 |
| Positive pole to ground | 75 | 74.94 | 0.060 | 0.0800 |
| | 50 | 49.97 | 0.025 | 0.0504 |
| | 25 | 25 | 0.002 | 0.0083 |
| Negative pole to ground | 75 | 74.94 | 0.060 | 0.0800 |
| | 50 | 50 | 0.002 | 0.0040 |
| | 25 | 24.96 | 0.041 | 0.0050 |

From the obtained results in Table 4, the maximum errors of determination of fault location using the proposed technique are:

- Pole-to-pole faults have a value of 0.10%,
- Positive pole-to-ground faults have a value of 0.08%,
- Negative pole-to-ground faults have a value of 0.04%,

These results prove the effectiveness of the proposed technique.

Table 5 presents the maximum error using this technique with a 100 Ω value of fault resistance and recently published methods.

Because the presented results are obtained from a MATLAB/Simulink simulation, the numerical values of the estimated fault distances should not be interpreted as representing the physical measurement resolution of a practical protection device. Therefore, the absolute fault-location error in kilometers and the corresponding percentage error are reported to provide a more meaningful assessment of the algorithmic accuracy.

The transmission medium investigated in this study is a 75 km bipolar HVDC cable. All fault-detection, fault-classification, and fault-location results presented in this work are obtained from this cable-based VSC-HVDC model. The proposed method is therefore validated for the specified cable model, while its applicability to overhead HVDC

lines requires additional investigation because of the differences in their propagation and frequency-dependent characteristics.

**Table 5.** Comparison between results of fault distance error from the proposed technique and recently published methods, with the effect of fault resistance.

| Reference | Fault Resistance (Ω) | Fault Distance Error % |
|---|---|---|
| [10] | 100 | 0.4 |
| [25] | 100 | 0.36 |
| [26] | Zero | 0.2 |
| [29] | 100 | 1.32 |
| [30] | 300 | 0.11 |
| [31] | 100 | 1 |
| [32] | Zero | 0.176 |
| The proposed technique | 100 | 0.10591 |

The 75 km fault case corresponds to a fault applied at the receiving-end boundary of the modeled 75 km transmission section. This case is included as an end-of-line test to examine the behavior of the proposed location algorithm close to the receiving terminal. It should therefore not be interpreted as an internal fault occurring beyond the physical boundary of the protected line.

The results obtained from the proposed technique show that its error is smaller than those reported in previous research.

## 7. Conclusions and Future Work

The proposed protection technique combines discrete wavelet transform of the pole-current signals with double-terminal traveling-wave analysis for fault classification and fault-location estimation in a bipolar VSC-HVDC system. The simulation results demonstrate the capability of the proposed approach to distinguish positive-pole-to-ground, negative-pole-to-ground, and pole-to-pole faults and to estimate their locations for the investigated 75 km HVDC cable model. The results also demonstrate that the fault-location error remains small for the investigated fault cases and fault resistance conditions. However, the sensitivity of the wavelet-coefficient criterion decreases as the fault distance increases, and the extended-distance results should therefore not be interpreted as validation for arbitrary transmission-line lengths. In addition, the present study does not systematically investigate heterogeneous line sections and multiple traveling-wave reflections. Future work will therefore focus on validating the proposed technique using different HVDC line lengths, voltage levels, cable and overhead-line configurations, and more detailed models incorporating complex reflection paths and practical network components.

This paper presented a novel protection technique for bipolar HVDC transmission lines based on double-terminal current traveling-wave analysis combined with discrete wavelet transform (db4) of pole currents. The method simultaneously addresses fault type classification and fault location determination, achieving a maximum location error of 0.11% even under fault resistances up to 100 Ω. Unlike machine-learning-based approaches, the proposed algorithm requires no prior training and maintains high accuracy across varying operating conditions, line lengths, and noise levels. Comparative evaluation with recently published methods confirm its superior accuracy and suitability for real-time implementation.

The key contributions of this work include: (i) a simple yet effective fault classification criterion using first-level DWT detail coefficients of positive, negative, and ground currents; (ii) this contradicts the method's use of double-terminal measurements (which require communication/synchronization); and (iii) demonstrated robustness under high-resistance faults, different fault types, and changing system parameters.

However, the study has certain limitations. The validation was performed on a specific 200 MVA, ±100 kV, 75 km bipolar VSC-HVDC model. Extension to multi-terminal HVDC grids, hybrid LCC-MMC topologies, and practical field implementation with synchronization considerations remains to be investigated. Future work will focus on hardware-in-the-loop validation, adaptation to different voltage levels and line configurations, and application of the proposed technique to high-voltage AC transmission systems.

The present study is simulation-based and experimental validation was not performed.

The present study is based on a uniform 75 km HVDC cable model and assumes that the first incident traveling-wave fronts can be reliably identified at the two terminals. Although smoothing reactors are included at the converter terminals, the effects of multiple reflections arising from line discontinuities, heterogeneous sections, converter-side components, and more complex HVDC network topologies have not been systematically investigated. These factors may influence traveling-wave propagation and the identification of the first wave front. Therefore, further studies using more detailed and heterogeneous HVDC network models are required to assess the robustness of the proposed technique under such conditions.

For future work, applying the proposed protection technique to high-voltage AC transmission systems is recommended.

A recommendation to extend the proposed technique to AC-side fault detection in hybrid AC/DC systems.

To demonstrate the effectiveness of the proposed technique, there must be Hardware-in-the-loop (HIL) testing and scaled-down laboratory prototype development.

**Author Contributions:** Conceptualization, A.S. (Abdelazim Salem) and W.M.; methodology, W.M. and A.S. (Abdellatif Sayed); software, W.M. and A.S. (Abdelazim Salem); validation, A.S. (Abdelazim Salem) and W.M.; formal analysis, S.H. and A.S. (Abdellatif Sayed); investigation, S.H. and W.M.; resources, S.H. and W.M.; data curation, W.M.; writing—original draft preparation, A.S. (Abdelazim Salem) and W.M.; writing—review and editing, A.S. (Abdelazim Salem) and A.S. (Abdellatif Sayed); visualization, W.M. and S.H.; supervision, S.H. and A.S. (Abdellatif Sayed). All authors have read and agreed to the published version of the manuscript.

**Funding:** This research received no external funding.

**Data Availability Statement:** The data of this research is available with the corresponding author if requested.

**Conflicts of Interest:** The authors declare no conflicts of interest.

## References

1. Zorig, A.; Belkheiri, M.; Barkat, S. Control of three-level T-type inverter based grid connected PV system. In *2016 13th International Multi-Conference on Systems, Signals & Devices (SSD)*; IEEE: Piscataway, NJ, USA, 2016; pp. 134–139. [CrossRef]
2. Eissa, M.M.; Hasan, S.; Mamdouh, R. Fault detection algorithm for multi-terminal LCC HVDC interconnected grid. *IOP Conf. Ser. Mater. Sci. Eng.* **2018**, *366*, 012066. [CrossRef]
3. Nagar, K.; Shah, M. A review on different ANN based fault detection techniques for HVDC systems. *Int. J. Innov. Res. Eng. Manag.* **2016**, *3*, 477–481. [CrossRef]
4. Torres, A.; Santos, R.C.D.; Yang, Q.; Li, J. Analyses of different approaches for detecting, classifying and locating faults in a three-terminal VSC-HVDC system. *Int. J. Electr. Power Energy Syst.* **2022**, *135*, 107514. [CrossRef]
5. Venkatesh, C.; Rao, P.V. Wavelet-ANN based classification of HVDC converter faults. In *2016 IEEE 6th International Conference on Power Systems (ICPS)*; IEEE: Piscataway, NJ, USA, 2016; pp. 1–6. [CrossRef]

6. Ahmed, N.; Ram, N.; Memon, A.P.; Ahmed, S. Comparative analysis of fault detection for HVDC transmission system using wavelet transform based on standard deviation. In *2020 3rd International Conference on Computing, Mathematics and Engineering Technologies (iCoMET)*; IEEE: Piscataway, NJ, USA, 2020; pp. 1–6. [CrossRef]
7. Alam, M.S.; AL-Ismail, F.S.; Abido, M.A.; Hossain, M.A. Fault current limiter of VSC-HVDC systems using variable resistive bridge controller. *Ain Shams Eng. J.* **2021**, *12*, 2643–2654. [CrossRef]
8. Hasan, S.; El-Refaie, E.-S.M.; Alaboudy, A.H.K.; Hamada, A.M. An AC hybrid current limiting and interrupting device for low voltage systems. *Alex. Eng. J.* **2017**, *56*, 1451–1460. [CrossRef]
9. Luo, S.; Dong, X.; Shi, S.; Wang, B. A directional protection scheme for HVDC transmission lines based on reactive energy. In *2016 IEEE Power and Energy Society General Meeting (PESGM)*; IEEE: Piscataway, NJ, USA, 2016; pp. 1–5. [CrossRef]
10. Saber, A. A backup protection algorithm for bipolar line-commutated converter HVDC lines. *IEEE Syst. J.* **2020**, *15*, 1172–1178. [CrossRef]
11. Syafiri, R.A.; Prasetyono, M.H.; Khafidli, M.K.; Anggriawan, D.O.; Tjahjono, A. Real-Time DC Arc Fault Detection Based on Fast Fourier Transform. In *2018 International Electronics Symposium on Engineering Technology and Applications (IES-ETA)*; IEEE: Piscataway, NJ, USA, 2018; pp. 1–5. [CrossRef]
12. Devadasu, G.; Sushama, M. A novel multiple fault identification with fast fourier transform analysis. In *2016 International Conference on Emerging Trends in Engineering, Technology and Science (ICETETS)*; IEEE: Piscataway, NJ, USA, 2016. [CrossRef]
13. Yeap, Y.M.; Ukil, A. Fault detection in HVDC system using Short Time Fourier Transform. In *2016 IEEE Power and Energy Society General Meeting (PESGM)*; IEEE: Piscataway, NJ, USA, 2016. [CrossRef]
14. Keshri, J.P.; Tiwari, H. Fault classification in VSC-HVDC transmission system using machine learning approach. In *2019 8th International Conference on Power Systems (ICPS)*; IEEE: Piscataway, NJ, USA, 2019; pp. 1–6. [CrossRef]
15. Chen, M.-J.; Lan, S.; Chen, D.-Y. Machine learning based one-terminal fault areas detection in HVDC transmission system. In *2018 8th International Conference on Power and Energy Systems (ICPES)*; IEEE: Piscataway, NJ, USA, 2018; pp. 1–6. [CrossRef]
16. Unal, F.; Ekici, S. A fault location technique for HVDC transmission lines using extreme learning machines. In *2017 5th International Istanbul Smart Grid and Cities Congress and Fair (ICSG)*; IEEE: Piscataway, NJ, USA, 2017; pp. 1–5. [CrossRef]
17. Fuentes-Burruel, J.M.S.; Moreno-Goytia, E.; Barajas, Á.C. Auxiliary short-circuit fault classification for HVDC systems based on VCO. In *2023 IEEE International Autumn Meeting on Power, Electronics and Computing (ROPEC)*; IEEE: Piscataway, NJ, USA, 2023; pp. 1–6. [CrossRef]
18. Dessouky, S.S.; Fawzi, M.; Ibrahim, H.A.; Ibrahim, N.F. DC pole to pole short circuit fault analysis in VSC-HVDC transmission system. In *Proceedings of the 2018 Twentieth International Middle East Power Systems Conference (MEPCON), Cairo, Egypt, 18–20 December 2018*; IEEE: Piscataway, NJ, USA, 2018; pp. 1–6. [CrossRef]
19. Li, Z.; Bai, G.; Hu, J.; Chen, H.; Xiong, X. Research on the short-circuit current of MMC-HVDC under DC pole-to-pole fault considering the impacts of DFIG. In *Proceedings of the 2023 3rd New Energy and Energy Storage System Control Summit Forum (NEESSC), Mianyang, China, 26–28 September 2023*; IEEE: Piscataway, NJ, USA, 2023. [CrossRef]
20. Huo, Q.; Lu, Y.; Su, Q.; Tang, X.; Ma, S.; Li, K.; Zhang, H. Short circuit current limiting method based on VSC-HVDC current limiting strategy. *IOP Conf. Ser. Earth Environ. Sci.* **2021**, *647*, 012139. [CrossRef]
21. Johnson, J.M.; Yadav, A. Complete protection scheme for fault detection, classification and location estimation in HVDC transmission lines using support vector machines. *IET Sci. Meas. Technol.* **2017**, *11*, 279–287. [CrossRef]
22. Chen, Z.; Zhou, Z.; Wang, X.; Li, Y.J.; Du, D.X.; Zhan, R.R.; Wang, S.Y. Traveling wave protection for hybrid HVDC transmission lines based on dual-tree complex wavelet transform. *Power Syst. Technol.* **2019**, *43*, 3832–3840.
23. Zhang, Y.; Wang, H.; Li, T.; Lin, Z.; Chang, Y. Combined single-end fault location method for LCC-VSC hybrid HVDC transmission line. *Autom. Electr. Power Syst.* **2019**, *43*, 187–194.
24. Zheng, X.; Nadeem, M.H.; Tai, N.; Habib, S.; Wang, B.; Yu, M.; He, Y. A transient current protection and fault location scheme for MMC-HVDC transmission network. *Int. J. Electr. Power Energy Syst.* **2021**, *124*, 106348. [CrossRef]
25. Swetapadma, A.; Agarwal, S.; Ranjan, A.; Abdelaziz, A.Y. A novel fault distance estimation method for voltage source converter-based HVDC transmission lines. *Electr. Power Compon. Syst.* **2021**, *48*, 1760–1772. [CrossRef]
26. Li, B.; Lv, M.; Li, B.; Xue, S.; Wen, W. Research on an improved protection principle based on differential voltage traveling wave for VSC-HVDC transmission lines. *IEEE Trans. Power Deliv.* **2020**, *35*, 2319–2328. [CrossRef]
27. Silva, A.S.; Santos, R.C.; Torres, J.A.; Coury, D.V. An accurate method for fault location in HVDC systems based on pattern recognition of DC voltage signals. *Electr. Power Syst. Res.* **2019**, *170*, 64–71. [CrossRef]
28. Xiao, H.; Ren, S.; Li, Y. Novel disturbance blocking criterion for reliable current differential protection of LCC-HVDC lines. *IEEE Trans. Power Deliv.* **2020**, *36*, 477–480. [CrossRef]
29. Azizi, S.; Sanaye-Pasand, M.; Abedini, M.; Hassani, A. A traveling-wave-based methodology for wide-area fault location in multiterminal DC systems. *IEEE Trans. Power Deliv.* **2014**, *29*, 2552–2560. [CrossRef]
30. Xing, L.H.; Chen, Q.; Xue, B.L. A fault location method for HVDC transmission lines. *Appl. Mech. Mater.* **2014**, *556–562*, 2723–2727. [CrossRef]

31. Octavio, J.; Torres, A.; Caneloi, R. New method based on wavelet transform and ANN for multiterminal HVDC system protection. In *2019 IEEE Milan PowerTech*; IEEE: Piscataway, NJ, USA, 2019; pp. 1–6.
32. Wang, D.; Fu, J.; Hou, M.; Qiao, F.; Gao, M. Novel travelling wave fault location principle for VSC-HVDC transmission line. *Electr. Power Syst. Res.* **2021**, *196*, 107226. [CrossRef]

**Disclaimer/Publisher's Note:** The statements, opinions and data contained in all publications are solely those of the individual author(s) and contributor(s) and not of MDPI and/or the editor(s). MDPI and/or the editor(s) disclaim responsibility for any injury to people or property resulting from any ideas, methods, instructions or products referred to in the content.